

Short Communication

Increased expression of Dsg2 in malignant skin carcinomas

A tissue-microarray based study

Donna Brennan and M G. Mahoney*

Department of Dermatology and Cutaneous Biology; Thomas Jefferson University; Philadelphia, PA USA

Abbreviations: Dsg2, desmoglein 2

Key words: carcinogenesis, desmoglein, desmosome, skin

Desmoglein 2 (Dsg2), a transmembrane cadherin of the desmosomal cell-cell adhesion structure, is downregulated with epithelial differentiation. We recently demonstrated that overexpression of Dsg2 in epidermal keratinocytes deregulates multiple signaling pathways associated with increased growth rate, anchorage-independent cell survival, and the development of skin tumors. While changes in Dsg2 expression have been observed in neoplastic lesions, the correlation of expression levels and localization of Dsg2 and the state of tumor development has not been fully established. Here we generated a highly sensitive Dsg2 antibody (Ab10) and characterized that antibody along with a previously developed Dsg2 specific antibody 10D2. Using these antibodies in immunostaining of tissue microarrays, we show a dramatic upregulation of Dsg2 expression in certain human epithelial malignancies including basal cell carcinomas (BCC; n = 12), squamous cell carcinomas (SCC; n = 57), carcinomas of sebaceous and sweat glands (n = 12), and adenocarcinomas (n = 3). Dsg2 expression was completely absent in malignant fibrosarcomas (n = 16) and melanomas (n = 15). While Dsg2 expression was consistently strong in BCC, it varied in SCC with a minor correlation between a decrease of Dsg2 expression and tumor differentiation. In summary, we have identified Dsg2 as a potential novel marker for epithelial-derived malignancies.

Introduction

Desmosomes are specialized intercellular structures that play vital roles in cell-cell adhesion and tissue integrity.¹ Loss of desmosomal adhesion is the underlying cause of several autoimmune, infectious and inherited diseases affecting diverse tissues such as the skin, hair and heart. Yet the components of these adhesive structures have also been implicated in the development or modulation of epithelial-derived tumors, thus highlighting complex roles of cell adhesion molecules in health and disease. Cell-cell contacts are often

reorganized during malignant transformation as evidenced by E- to P- or N-cadherin switch.^{2,3} Although desmosome assembly is also frequently impaired in tumor cells, there is conflicting evidence as to what role desmosomal adhesion and/or desmosomal components play in carcinogenesis.⁴ Some studies show increased expression of desmosomal components in highly invasive cancers while others demonstrate enhanced desmosome disassembly in some advanced epithelial cancers.

It is generally thought that invasion and metastasis of malignant cells is facilitated in part through the loss of cell-cell adhesion. The loss of E-cadherin expression is frequently observed in multiple epithelial tumors.^{1,4} Desmosomal adhesion has been considered in a similar vein based on evidence of loss of heterozygosity (LOH) at chromosome 18q12 (region of desmosomal cadherin gene cluster) in many cancers including squamous cell carcinomas (SCC). Furthermore, this LOH is frequently correlated with poor prognosis in advanced tumor stage.^{5,6} However, the relationship between loss of desmosomal adhesion and clinical outcomes of epithelial neoplasia is less clear. Several investigators reported loss of either desmosomes or desmosomal structural components in epithelial malignancies including SCC;⁷⁻⁹ whereas others observed no statistically significant relationships between loss of desmosomal components (desmoplakin and desmoglein) and prognosis in patients with head and neck SCC, although loss of E-cadherin was strongly linked to recidivism and poor prognosis in this cohort of patients.¹⁰

There are four distinct desmoglein genes (Dsg1, Dsg2, Dsg3 and Dsg4), each differentially expressed depending upon the type of tissue and the state of differentiation. Although the role of desmogleins in cell-cell adhesion has been well studied, their individual roles in carcinogenesis are poorly understood.^{7,11} Early studies looking at desmoglein expression in cancers yielded conflicting results, due to the use of antibodies that cross-reacted with multiple isoforms. However, when isoform-specific antibodies are used, a different picture begins to emerge. Studies with Dsg2-specific antibodies have demonstrated that Dsg2 is strongly expressed in high risk SCC of the skin.¹² This study reinforces earlier research revealing strong and consistent expression of Dsg2 in human SCC.¹³ Additionally, Dsg2 is highly expressed in carcinoma cell lines derived from both simple and complex epithelia, but not in normal epithelial cells, possibly reflecting tumor cell kinetics such as cell invasion and metastasis.¹³⁻¹⁵ Dsg2 has also been implicated in other carcinomas. Genetic profiling

*Correspondence to: M G. Mahoney; Department of Dermatology and Cutaneous Biology; Jefferson Medical College; 233 S. 10th Street; Suite 428 BLSB; Philadelphia, PA 19107 USA; Tel.: 215.503.3240; Fax: 215.503.5788; Email: my.mahoney@jefferson.edu

Submitted: 10/28/08; Accepted: 12/04/08

Previously published online as a *Cell Adhesion & Migration* E-publication: <http://www.landesbioscience.com/journals/celladhesion/article/7539>

of epithelial-derived prostate cancer cell lines showed increased expression of Dsg2 in a metastatic cell line as compared to its non-metastatic syngeneic precursor cell.¹⁶ In esophageal carcinomas, Dsg1 and Dsg2 are not reduced in expression, but rather redistributed to the cytoplasm or perinuclear region. Interestingly, similar results are observed in gastric cancers where Dsg2 is enhanced and often aberrantly expressed in the cytoplasm.¹⁷ The most compelling recent finding shows Dsg2 as the sole desmosomal cadherin highly expressed in malignant melanoma cell lines with diffuse staining over the cell surface of the cell in a non-junction-restricted form.¹⁸ Finally, our laboratory recently observed hyperproliferation, epidermal thickening and formation of benign tumors (papillomas) in the epidermis of transgenic mice overexpressing Dsg2.¹⁹ Taken together these results support a role for Dsg2 in epithelial tumor development.

Results and Discussion

Tumor tissues are often fixed, processed and stored in formalin and embedded in paraffin, a process that utilizes extensive cross-linking of proteins, which often results in the loss of conformational epitopes. Thus, to assess the expression level of Dsg2 in these tissue samples we set out to establish antibodies that are functional in formalin/paraffin tissues. We first generated recombinant glutathione S-transferase (GST) fusion proteins of the extracellular domains (EC1-5) of Dsg2 (Fig. 1A and B) and immunoblotting analysis using antibodies against GST detected all Dsg2-EC-GST fusion proteins (Fig. 1B). Based on the amino acid sequence, we raised antibodies against the EC5 domain as this domain shares the least homology with other desmosomal cadherins.²⁰ We produced two polyclonal antibodies (Ab9 and Ab10) in rabbits. To confirm the specificity and map these antibodies, we performed immunoblotting using the Dsg2-EC-GST-fusion proteins (Fig. 1B). In addition to our antibodies, we also obtained several antibodies specific against Dsg2 including 10D2, Rb5, 10G11, 6D8, H-145 and DG3.10. Western blotting results are as follows: 10D2 to EC1; Rb5 to EC2-3; 10G11 to EC3; 6D8 to EC4; Ab10 and Ab9 (not shown) to EC5. Since Ab10, but not Ab9, recognized Dsg2 in formalin-fixed paraffin-embedded tissues, it was used in the remainder of this study. We note here that stringent protocols used to purify GST fusion proteins in bacteria resulted in some proteolytic processing or degradation. Thus, sensitive antibodies such as Rb5 or Ab10 may detect these degradative products as multiple bands on a western blot (Fig. 1B). Finally, Rb5 is a polyclonal antibody and thus likely contains two populations of antibodies, one recognizing the EC2 and the other recognizing the EC3 domains.

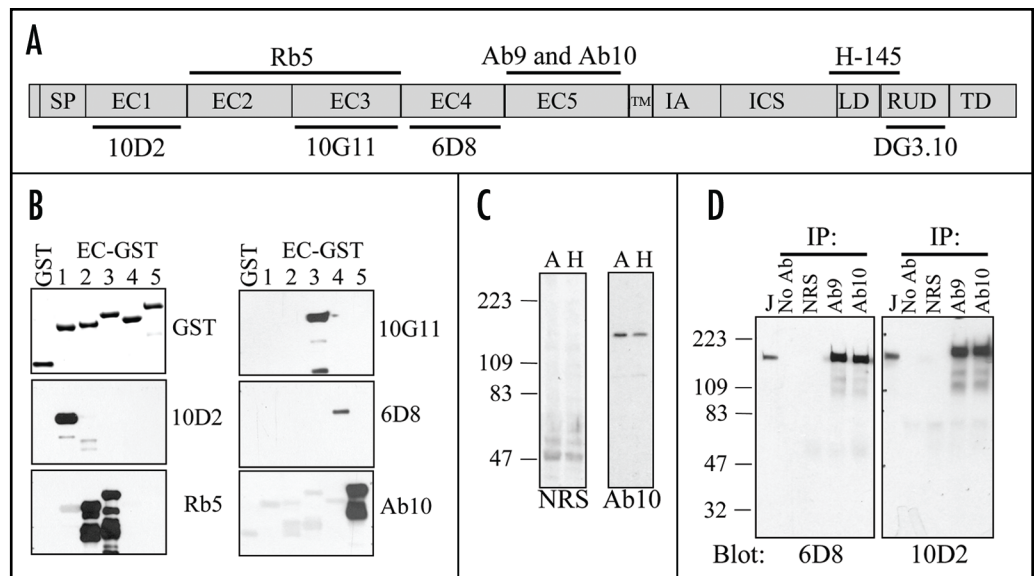


Figure 1. Characterization of our panel of Dsg2 specific antibodies. (A) Schematic diagram of the structural domains of Dsg2 and the putative recognition sites of the various Dsg2 antibodies. SP, signal peptide; EC, extracellular domain; TM, transmembrane; IA, intracellular anchoring; ICS, intracellular cadherin segments; LD, linker domain; RUD, repeat unit domain; TD, terminal domain. (B) We generated GST fusion proteins of Dsg2 extracellular domains (EC, 1–5), purified, resolved over SDS-PAGE, and subjected them to immunoblotting analysis with antibodies against GST and Dsg2. Recognition results as follows: 10D2 to EC1; Rb5 to EC2/3; 10G11 to EC3; 6D8 to EC4; and Ab10 to EC5. (C) Total cellular protein was extracted from A431 (A) and HaCaT (H) cells, resolved over SDS-PAGE and immunoblotted with normal rabbit serum (NRS; 1:10,000) or Ab10 (1:100,000). A band ~160 kDa was detected in both A431 and HaCaT cells. (D) Dsg2 was immunoprecipitated from JAR cells extracted in RIPA buffer with no antibody (No Ab), normal rabbit serum (NRS), antibody 9 (Ab9), or antibody 10 (Ab10). The immunoprecipitates were immunoblotted with Dsg2 specific antibodies 6D8 or 10D2. Total cell lysate was used as control (J).

Next, to detect intact Dsg2 with Ab10 we immunoblotted total protein lysates from epithelial A431 and HaCaT cells. Ab10 (1:100,000) detected a protein approximately 150–160 kDa, the observed full length Dsg2 protein (predicted MW of Dsg2 protein is approx 122 kDa) in both A431 and HaCaT cells. The normal rabbit serum (NRS; 1:10,000) did not detect any proteins that size. To further confirm the specificity of Ab10, we performed immunoprecipitation using total protein lysates from human choriocarcinoma (JAR) cells, which express high level of Dsg2 (not published). The precipitated products along with total JAR cell lysates were immunoblotted with Dsg2 antibodies 6D8 and 10D2 (Fig. 1D). Both 6D8 and 10D2 antibodies recognized a protein approximately 160 kD in the JAR cell lysate. A protein of comparable size was detected in samples precipitated in with Ab10 and Ab9 but not in the NRS or no antibodies (Fig. 1D). In summary we have generated a polyclonal antibody specific against the EC5-domain of Dsg2.

We rule out cross-reactivity of Ab10 to Dsg3 by immunoblotting. Ab10 only recognized one band at approximately 150–160 kDa in A431 and HaCaT cells. Both cell lines express Dsg3, which is detected by immunoblotting at approximately 130–140 kDa. Furthermore, in human epidermis Dsg3 expression extends from the basal into the spinous layers, whereas Dsg2 expression is limited to the basal cell layer as detected by Ab10.

Next we performed immunostaining of normal adult skin using 10D2 and Ab10. The immunofluorescence intensity was graded on a semi-quantitative scale from 0 to 4 (score 0, no staining; score 1, faint above background staining; score 2, faint but distinct staining;

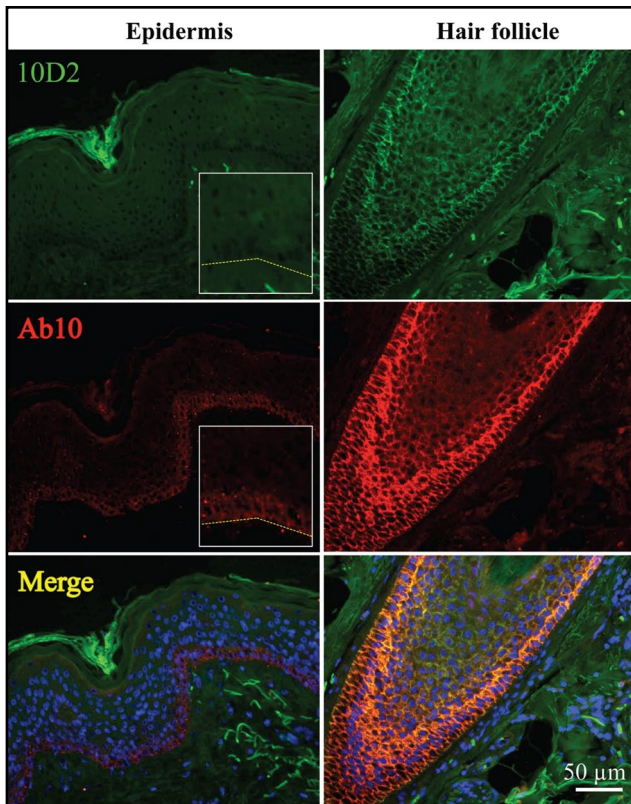


Figure 2. Dsg2 expression in the hair follicle. Immunostaining of Dsg2 using antibodies 10D2 (green) and Ab10 (red) in the adult epidermis and hair follicles showing faint Dsg2 expression in the basal cell layer of the epidermis and clear cell-cell border staining of the follicular outer-root-sheath cells.

score 3, moderate intensity; score 4, strong intensity) by two different individuals. Antibody 10D2 detected an insignificant level of Dsg2 in the epidermis (score 0), but robust expression was observed in hair follicles (score 4, Fig. 2). Our highly sensitive Ab10 showed faint staining of Dsg2 in the basal cell layer of the epidermis (score 1) and distinct cell-cell border staining in the hair follicle (score 4, Fig. 2). Merged image showed co-localization of 10D2 and Ab10 in the outer-root-sheath of the hair follicles. We note here that immunofluorescent staining with Ab10 is consistent with previously characterized Dsg2 antibodies, in that cell-cell border staining is restricted to the basal layer of the epidermis with highest levels in normal newborn foreskin but diminished in adult skin.²¹

Next we examined the expression of Dsg2 in a tissue panel of malignant skin tumors from Cybrdi (Fig. 3). The immunofluorescence intensity was graded and summarized in Table 1. Similar results were observed with both Ab10 and 10D2 performed on 2 different sets of tissue panels. We first examined the expression level of Dsg2 in the two major forms of skin cancers, basal cell carcinomas (BCC) and SCC, arising from either the basal cell layer or the differentiating cell layers, respectively.²² Since Dsg2 is normally expressed in the basal cell layer, we predicted a high expression of Dsg2 in BCC. Indeed, all 12 BCC presented expressed significantly high level of Dsg2 (Fig. 3 and Table 1). We also detected increased Dsg2 expression in SCC (n = 13), adenocarcinomas (n = 3) and glandular (sebaceous and sweat) carcinomas (n = 12) (Fig. 3 and Table 1). In adenocarcinomas, high level of Dsg2 was observed in ductal cells and the apical region of secretory cells. Virtually no Dsg2

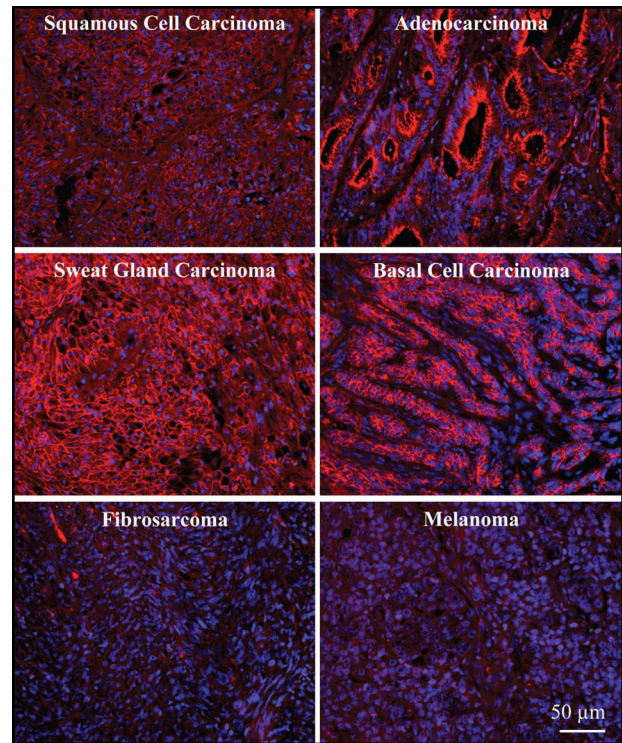


Figure 3. Enhanced staining of Dsg2 in skin carcinomas. Immunostaining of Dsg2 in a tissue array of malignant skin carcinomas showing dramatic high expression of Dsg2 (red) in squamous and basal cell carcinomas, glandular (sebaceous and sweat glands) carcinomas and adenocarcinomas, but not fibrosarcomas or melanomas.

staining was observed in fibrosarcomas (n = 16). Recent findings show Dsg2 highly expressed in 2 of 8 cultured melanoma cell lines with diffuse staining over the cell surface in a non-junction-restricted form.¹⁸ However using the Cybrdi panel, we did not detect any Dsg2 staining in malignant melanomas (n = 15). Given the small sample size of both studies, further analysis is needed to reconcile these in vitro and in vivo results. We note here that the representative stainings shown in Figure 3 would be scored the following: SCC, adenocarcinoma, sweat gland carcinoma and BCC, score 4; fibrosarcoma and melanoma, score 0.

In addition to enhanced level of Dsg2 expression, abnormal distribution in the cytoplasm, perinuclear region and nucleus was also previously observed in high risk SCC.¹² Upon further examination of the Dsg2 staining in our SCC, we observed the presence of Dsg2 in both the nuclei (arrows, Fig. 4A and B, score 2) and cytoplasm (Fig. 4C and D, score 3). The cytoplasmic staining was either diffuse (Fig. 4A) or punctuated (arrow head, Fig. 4C). While the nuclear staining of Dsg2 is infrequent and lacking in intensity, it is observed in multiple tumor samples. These results are further supported by our recent finding of Dsg2 in the cytoplasmic and nuclear fractions of skin lysates from transgenic mice overexpressing Dsg2.¹⁹ Additionally, nuclear transportation and localization of E-cadherin has been reported.²³⁻²⁵ Taken together, these results provide convincing evidence for the validity of nuclear localization of Dsg2 although the exact mechanism by which Dsg2 is transported into the nucleus remains to be determined. It is of intense interest what functions Dsg2 serves outside of the desmosomes.

Due to lack of available protein lysates of these tumor samples for immunoblotting, we performed quantitative analysis of immunofluorescent intensity. Measurements of fluorescent intensity of Dsg2 were performed with Image-Pro Plus image processing & analysis software (Media Cybernetics). Intensity was measured in small representative regions (63 x 101 pixels (0.2 x 0.3 inches); Table 2) or from the entire image (1275 x 1024 pixels (4.3 x 3.4 inches); Table 3). Our rationale for measuring fluorescent intensity using two different methods is as follows. First, in comparing with the skin and hair follicle where Dsg2 is differentially expressed in diverse cell compartments such as the basal but not suprabasal layers. The most appropriate method would be to measure a small area (0.2 x 0.3 inches) highlighting these specific compartments that are positive or negative for staining. Each data point is an average of at least four different representative readings. Secondly, to minimize researcher bias, we also measured the fluorescent intensity in the entire image (4.3 x 3.4 inches). Results shown in Table 3. Values for Table 2 are plotted in Figure 5. Fluorescent level in the superficial epidermis of normal human skin where Dsg2 was not expressed was used as baseline level for negative control. To determine statistical significance of the measured fluorescent values, we performed 2-tailed Student's t-test in Microsoft Excel program. Compared to the superficial epidermis (42.9 ± 10.9), there was no difference in the basal layer of the adult skin (48.4 ± 5.1); however Dsg2 fluorescent levels were significantly higher in the basal cell layer of palm skin (91.1 ± 12.3), hair follicles (164.5 ± 15.8), SCCs (98.3 ± 36.9), glandular carcinomas (97.7 ± 42.8) and BCCs (157.2 ± 39.6) but not fibrosarcomas (46.4 ± 8.1) or melanomas (42.5 ± 9.5) (Table 2). To further evaluate Dsg2 expression only in the skin tumors, we measured the fluorescent intensity from the entire images taken. Results demonstrate that in skin tumors, Dsg2 expression level was upregulated in carcinomas compared to fibrosarcomas or melanomas (Table 3).

While Dsg2 expression was consistently intense in BCCs, its expression was more varied in SCCs. To further assess Dsg2 expression with clinical classification, we immunostained a panel of SCCs and normal tissues from Imgenex with Ab10 and 10D2 (Table 4). Only 33% ($n = 9$) of normal human epidermis showed minor Dsg2 staining. On the other hand, 77% ($n = 44$) SCCs showed high level of Dsg2 expression, which correlated with the differentiation state of the tumor. While 100% ($n = 4$) of poorly differentiated SCCs showed intense +4 staining, only 10% ($n = 20$) of well-differentiated SCCs received that score (Table 4). Interestingly all recurring SCCs ($n = 8$) while only half of metastatic SCCs ($n = 6$) expressed Dsg2. These results demonstrate a potential correlation between Dsg2 expression and poorly differentiated and recurring SCCs.

The current dogma in cancer biology is that cell adhesion is reduced during malignant transformation, in turn allowing malignant cells to migrate, invade and metastasize. However, we have demonstrated here that Dsg2 is highly upregulated in epithelial-derived skin tumors including SCC and BCC; and thus, have identified Dsg2 as a potential novel marker for skin malignant progression. These results support our recent published findings that transgenic mice overexpressing Dsg2 in the epidermis developed hyperplasia and spontaneous tumors and were more susceptible to chemical carcinogen-induced tumorigenesis.¹⁹ Furthermore, Dsg2 overexpression activated signaling pathways such as PI3K/Akt, MAPK, STAT3 and NFκB signaling pathways, which are often involved in cell

Table 1 Dsg2 expression in malignant skin tumors

Malignant skin tumors	Dsg2					total
	0	+1	+2	+3	+4	
Squamous cell carcinomas	1	3	2	3	4	13
Adenocarcinomas	0	0	0	2	1	3
Gland carcinomas	1	0	4	5	2	12
Basal cell carcinomas	0	0	2	4	6	12
Fibrosarcomas	16	0	0	0	0	16
Melanomas	15	0	0	0	0	15

Semi-quantitative assessment, 0, +1, +2, +3, +4.

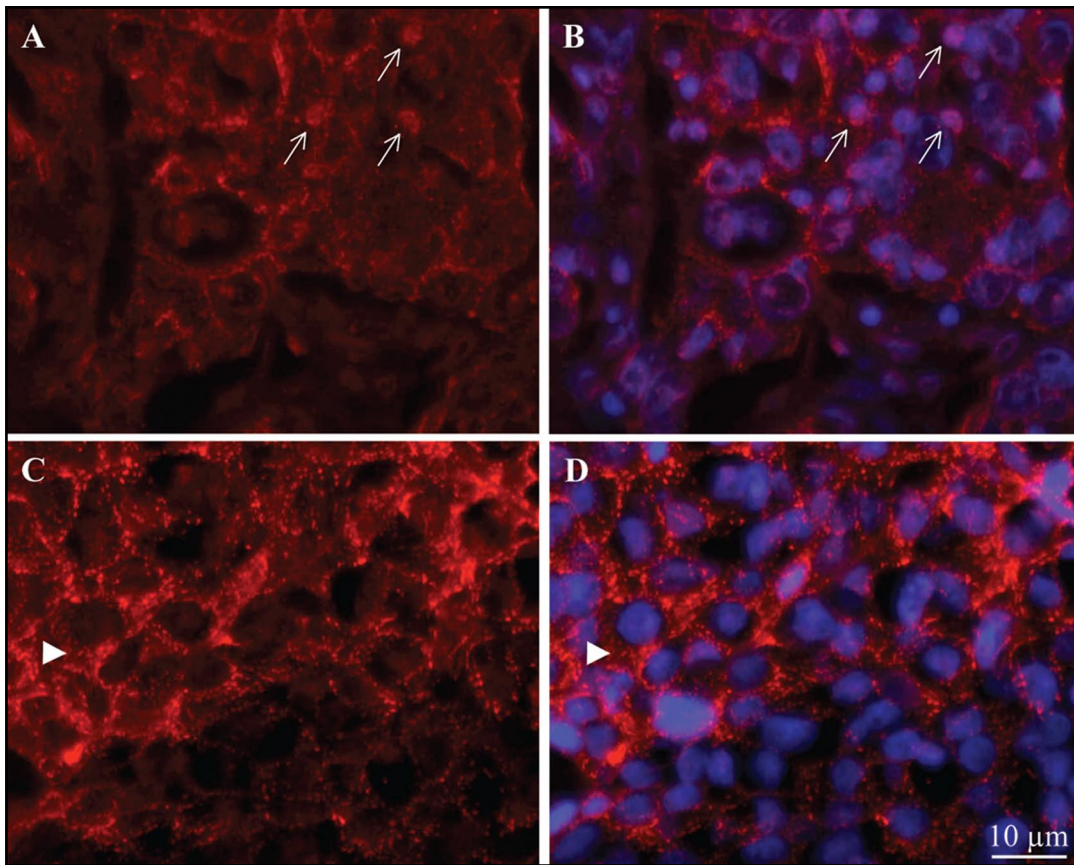
proliferation and survival. Taken together these results reinforce our hypothesis that Dsg2 supports some aspect of epithelial tumor development. However, we cannot rule out the possibility that the adhesive properties of Dsg2-containing desmosomes may be lower than that of Dsg1-containing desmosomes. Taken in conjunction with our report and others demonstrating enhanced and aberrant expression of Dsg2 in carcinomas, we cannot fully delineate the roles of Dsg2-mediated signaling and altered desmosomal adhesion in carcinomas. This report is part of a broader study in which we are characterizing desmoglein expression in skin carcinomas; work is currently in progress to optimize antibodies compatible with paraffin-embedded formalin-fixed tissue samples.

In summary this data identifies Dsg2 as a potential marker for a variety of skin-derived carcinomas. Furthermore, these results are the first step to defining a desmosomal cadherin profile to complement existing classical cadherin profiles to provide a more definitive picture of the role of adhesion molecules in cancer. Finally, these results will provide insights into the processes involved in malignant transformation, enabling us to identify targets for future mechanistic studies.

Materials and Methods

Antibodies. Antibodies used were: 10D2 and 6D8 (Dr. James Wahl, University of Nebraska Medical Center, Omaha, NE; 1:2 for immunofluorescence and 1:100 for western);^{26,27} Rb5 (Dr. Lutz Langbein, German Cancer Research Center, Heidelberg, Germany; 1:1,000 for immunofluorescence and 1:10,000 for western), 10G11 (Acris Antibodies, Hiddenhausen, Germany; 1:100 for immunofluorescence and 1:1,000 for western), H-145 (Santa Cruz Biotech, Santa Cruz, CA; 1:200 for immunofluorescence and 1:1,000 for western), and DG3.10 (Progen, Heidelberg, Germany; 1:200 for immunofluorescence and 1:1,000 for western). Alexa Fluor-conjugated secondary antibodies (488 and 594 nm) were from Molecular Probes (1:200; Eugene, OR).

Glutathione S-transferase fusion proteins. GST fusion proteins were produced and affinity purified on glutathione Sepharose beads according to the manufacturer (GE Healthcare, Piscataway, NJ) and as previously described.²⁸ GST-fusion proteins were obtained by in-frame cloning the extracellular (EC) domains of human *Dsg2* cDNAs into pGEX-4T-1 (GE Healthcare). Primers to generate Dsg2 EC domains were: EC1, forward 5'-ATG GCG CGG ACG CGG GAC-3' and reverse 5'-GCG CTT TTG CCG CAC TAA-3'; EC2, forward 5'-GCC TGG ATC ACC GCC CCC-3' and reverse 5'-GAA CAC TGG TTC GTT GTC-3'; EC3, forward 5'-ACA CAG GAT GTC TTT GTT-3' and reverse 5'-TAC TAC AGG



©2009 Landes Bioscience.

Figure 4. Subcellular distribution of Dsg2 in SCC. Immunostaining of Dsg2 in malignant skin carcinomas showing clear cell-membrane staining, aberrant localization of Dsg2 in the nuclei (arrows, A and B), and either diffuse or punctate cytoplasmic (arrow head, C and D) staining. Two representative images are shown. Blue, DAPI stained nuclei.

Table 2 Enhanced expression of Dsg2 in select skin tumors

Tumor	Mean \pm Std	p value
Superficial epidermis	42.9 \pm 10.9	-
Basal-skin	48.4 \pm 5.1	0.16
Basal-palm	91.1 \pm 12.3	0.00017*
Hair follicle	164.5 \pm 15.8	9.1 $\times 10^{-6}$ *
Fibrosarcoma	46.4 \pm 8.1	0.28
Melanoma	42.5 \pm 9.5	0.90
SCC	98.3 \pm 36.9	1.7 $\times 10^{-15}$ *
Glandular carcinoma	97.7 \pm 42.8	7.6 $\times 10^{-15}$ *
BCC	157.2 \pm 39.6	6.9 $\times 10^{-30}$ *

Performed 2-Tailed heteroscedastic Student's t-test. *p < 0.05 statistically significant.

Table 3 Enhanced expression of Dsg2 in skin carcinomas relative to fibrosarcomas and melanomas

Tumor type	N	Mean \pm Std	p value
Fibrosarcoma/Melanoma	31	43.8 \pm 7.9	-
SCC	13	62.5 \pm 22.5	0.012*
Glandular carcinoma	12	60.4 \pm 21.2	0.021*
BCC	12	99.7 \pm 25.6	0.000009*

Performed 2-Tailed heteroscedastic Student's t-test. *p < 0.05 statistically significant.

TAT ATT GTC-3'; EC4, forward 5'-GAA AAT AAA GTG CTT GAA-3' and reverse 5'-AAA ATG AAT GCC TTC TTT-3'; EC5, forward 5'-AAA AGC AGC GTC ATC TCA-3' and reverse 5'-CAG GCC CAC ATA GGA GTC-3'. The PCR amplified products were digested with *EcoRI* and *SalI* and inserted in frame into pGEX-4T-1. GST fusion proteins were produced in BL21 *E. coli* cells after induction with isopropyl-beta-D-thiogalactoside (0.5 mM). Cells were suspended in STE buffer (10 mM Tris, pH 8.0, 150 mM NaCl, 10 mM EDTA, 1% Triton X-100, 2% Sarcosyl, 1 mM DTT) with phenylmethylsulfonyl fluoride (1 mM). GST fusion proteins were clarified by centrifugation at 15,000 rpm for 20 min at 4°C and bound to Glutathione Sepharose beads and eluted with glutathione elution buffer according to the manufacturer's protocol (GE Healthcare). The eluted proteins were dialyzed against PBS and concentration was determined by Pierce BCA protein assay (Pierce Biotech, Rockford, IL).

Preparation of anti-Dsg2 antiserum. Dsg2-EC5-GST recombinant protein was conjugated to keyhole limpet hemocyanin and used to immunize male New Zealand rabbits by CoCalico Biologicals (Reamstown, PA) to generate antibodies Ab9 and Ab10. To affinity purify Ab10, we cross-linked 1 mg of GST and Dsg2-EC5-GST proteins to 5 ml of Affigel-10 (Bio-Rad Labs, Hercules, CA) according to the manufacturer's protocol. Crude serum was passed through the GST column to remove non-specific antibodies. The flow-through material was added to the Dsg2-EC5-GST column

and incubated for 2 hr to room temperature. The column was then washed with PBS, 20 times column bed volume, and antibodies were eluted using ImmunoPure IgG elution buffer (Pierce Biotech).

Immunoprecipitation, immunoblotting and immunohistochemistry. Immunoblotting was performed as described previously with 0.2 µg of GST or 20 µg cellular protein in each lane resolved over 10% SDS-PAGE (Bio-Rad Labs).^{19,29} Signals were detected with chemiluminescence (ECL; GE Healthcare).

For immunoprecipitation, confluent monolayer of JAR cells were rinsed three times with phosphate buffered saline (PBS) and extracted in RIPA buffer (50 mM Tris (pH 7.5), 150 mM NaCl, 1% Nonidet P-40, 0.5% deoxycholate, 0.1% SDS, 1 mM DTT, protease inhibitor cocktail (Roche Diagnostic, Indianapolis, IN) and 2 mM PMSF. Insoluble material was discarded after centrifugation at 14,000 xg for 15 min at 4°C. Cell lysate was incubated with 10 µl of antibodies and 50 µl protein A/G agarose (Pierce Biotech) at 4°C for 2 hrs. Immune complexes were washed five times with TBST (10 mM Tris-HCl, pH7.5, 150 mM NaCl and 1% Tween-20). Beads were boiled in Laemmli sample buffer and proteins were resolved by SDS-PAGE for immunoblotting analysis.

For immunohistochemistry, tissue sections (4 µm) from formalin-fixed and paraffin-embedded tissues were used as described previously.^{19,21,29} We used two tissue arrays of skin tumors (squamous carcinoma, adenocarcinoma, basal cell carcinoma, sarcoma and melanoma) of different grades and matching normal adjacent tissues (paraffin-embedded) from Imgenex (Catalog # IMH-323; San Diego, CA) and Cybrdi Cybrdi (Catalog # CC21-01-001; Frederick, Maryland). Tissue sections were deparaffinized in 100% xylene (5 min; 2 times), 100% ethanol (5 min; 2 times), 95% ethanol (5 min; 2 times), 75% ethanol (2 min), 50% ethanol (2 min) and H₂O (2 min). Antigen retrieval was performed by the microwave method with sodium citrate followed by digestion with trypsin (Sigma, St. Louis, MO) for 10 min at 42°C. Nonspecific binding sites were blocked with 5% normal goat serum, 1% BSA and 0.02% TX-100 in PBS and primary and secondary antibodies were incubated in blocking buffer. Nuclei were stained with DAPI (Sigma) prior to mounting for viewing under fluorescence microscope. All fluorescent images were acquired using a Hamamatsu monochromatic digital camera (Phase 3 Imaging Systems, Glen Mills, PA, USA; C4742-95) and analyzed using Image Pro 6.1 imaging software (Media Cybernetics, Bethesda, MD, USA). Select areas of interest (either 63 x 101 or 1,024 x 1,275 pixels) were evaluated for mean signal intensity. Statistical analysis of the data was performed in Microsoft Excel.

Acknowledgements

We thank Drs. Lutz Langbein (German Cancer Research Center, Heidelberg, Germany) for the Rb5 antibody and James Wahl

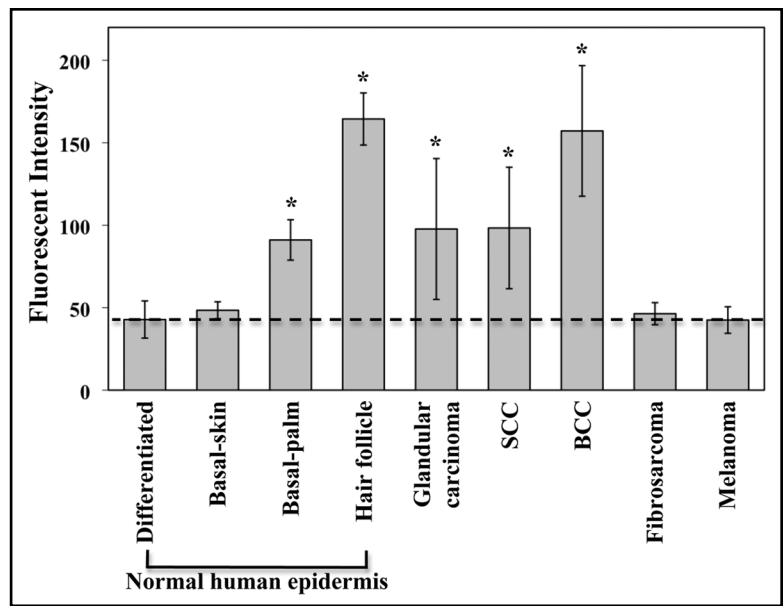


Figure 5. Comparison of Dsg2 expression in normal skin and skin tumors. Dsg2 fluorescent intensity levels were measured in 63 x 101 pixels (0.2 x 0.3 inches) using Image-Pro Plus image processing & analysis software (Media Cybernetics). In the normal skin, fluorescent intensity was measured in the basal and superficial (differentiated) epidermis and hair follicles. Dashed line demarcates fluorescent intensity measured in the differentiated epidermis where Dsg2 is not expressed. Results summarized in Table 2. Values given as Mean ± Std. *p ≤ 0.05.

Table 4 Expression profiles of Dsg2 in normal skin and SCC

Dsg2	Pathology (subtype)			Histology (differentiation state)				
	NHS (n=9)	SCC (n=44)	SCC (n=30)	Recurring (n=8)	Metastatic (n=6)	Poor (n=4)	Moderate (n=7)	Well (n=20)
0	6	10	7	0	3	0	1	5
+1	1	8	6	1	1	0	2	6
+2	2	6	5	1	0	0	1	3
+3	0	7	5	1	1	0	1	4
+4	0	13	7	5	1	4	2	2
Positive staining	3/9* (33%)	34/44** (77%)	23/30 (77%)	8/8 (100%)	3/6 (50%)	4/4 (100%)	6/7 (86%)	15/20 (75%)

Semi-quantitative assessment, 0, +1, +2, +3, +4. *Staining restricted to the basal cell layer in the interfollicular epidermis. **Staining extensive throughout tumor mass. NHS, normal human skin; SCC, squamous cell carcinoma.

(University of Nebraska Medical Center, Omaha, NE) for the antibodies 6D8 and 10D2. This work was supported by a grant (Mahoney, AR055251) from the National Institutes of Health.

References

- Holthöfer B, Windoffer R, Troyanovsky S, Leube RE. Structure and function of desmosomes. *Int Rev Cytol* 2007; 264:65-163.
- Stefansson IM, Salvesen HB, Akslen LA. Prognostic impact of alterations in P-cadherin expression and related cell adhesion markers in endometrial cancer. *J Clin Oncol* 2004; 22:1242-52.
- Gravdal K, Halvorsen OJ, Haukaas SA, Akslen LA. A switch from E-cadherin to N-cadherin expression indicates epithelial to mesenchymal transition and is of strong and independent importance for the progress of prostate cancer. *Clin Cancer Res* 2007; 13:7003-11.
- Chidgey M, Dawson C. Desmosomes: a role in cancer? *Br J Cancer* 2007; 96:1783-7.
- Petersen S, Aninat-Meyer M, Schluns K, Gellert K, Dietel M, Petersen I. Chromosomal alterations in the clonal evolution to the metastatic stage of squamous cell carcinomas of the lung. *Br J Cancer* 2000; 82:65-73.

6. Takebayashi S, Ogawa T, Jung KY, Muallem A, Mineta H, Fisher SG, et al. Identification of new minimally lost regions on 18q in head and neck squamous cell carcinoma. *Cancer Res* 2000; 60:3397-403.
7. Kronic AL, Garrod DR, Madani S, Buchanan MD, Clark RE. Immunohistochemical staining for desmogleins 1 and 2 in keratinocytic neoplasms with squamous phenotype: actinic keratosis, keratoacanthoma and squamous cell carcinoma of the skin. *Br J Cancer* 1998; 77:1275-9.
8. Shinohara M, Hiraki A, Ikebe T, Nakamura S, Kurahara S, Shirasuna K, et al. Immunohistochemical study of desmosomes in oral squamous cell carcinoma: correlation with cytokeratin and E-cadherin staining, and with tumour behaviour. *J Pathol* 1998; 184:369-81.
9. Matsumoto M, Natsugoe S, Nakashima S, Shimada M, Nakano S, Kusano C, et al. Biological evaluation of undifferentiated carcinoma of the esophagus. *Ann Surg Oncol* 2000; 7:204-9.
10. Bosch FX, Andl C, Abel U, Kartenbeck J. E-cadherin is a selective and strongly dominant prognostic factor in squamous cell carcinoma: a comparison of E-cadherin with desmosomal components. *Int J Cancer* 2005; 114:779-90.
11. Pittella F, Katsube K, Takemura T, Hashimoto T, Kawano T, Garrod D, et al. Perinuclear and cytoplasmic distribution of desmoglein in esophageal squamous cell carcinomas. *Pathol Res Pract* 2001; 197:85-91.
12. Kurzen H, Munzing I, Hartschuh W. Expression of desmosomal proteins in squamous cell carcinomas of the skin. *J Cutan Pathol* 2003; 30:621-30.
13. Harada H, Iwatsuki K, Ohtsuka M, Han G, Kaneko F. Abnormal desmoglein expression by squamous cell carcinoma cells. *Acta Derm Venereol* 1996; 76:417-20.
14. Denning MF, Guy SG, Ellerbroek SM, Norvell SM, Kowalczyk AP, Green KJ. The expression of desmoglein isoforms in cultured human keratinocytes is regulated by calcium, serum and protein kinase C. *Exp Cell Res* 1998; 239:50-9.
15. Schäfer S, Stumpp S, Franke WW. Immunological identification and characterization of the desmosomal cadherin Dsg2 in coupled and uncoupled epithelial cells and in human tissues. *Differentiation* 1996; 60:99-108.
16. Trojan L, Schaaf A, Steidler A, Haak M, Thalmann G, Knoll T, et al. Identification of metastasis-associated genes in prostate cancer by genetic profiling of human prostate cancer cell lines. *Anticancer Res* 2005; 25:183-91.
17. Biedermann K, Vogelsang H, Becker I, Plaschke S, Siewert JR, Hofler H, et al. Desmoglein 2 is expressed abnormally rather than mutated in familial and sporadic gastric cancer. *J Pathol* 2005; 207:199-206.
18. Schmitt CJ, Franke WW, Goerdts S, Falkowska-Hansen B, Rickett S, Peitsch WK. Homotypic and heterotypic cell contacts in malignant melanoma cells and desmoglein 2 as a novel solitary surface glycoprotein. *J Invest Dermatol* 2007; 127:2191-206.
19. Brennan D, Hu Y, Joubeh S, Choi YW, Whitaker-Menezes D, O'Brien T, et al. Suprabasal Dsg2 expression in transgenic mouse skin confers a hyperproliferative and apoptosis-resistant phenotype to keratinocytes. *J Cell Sci* 2007; 120:758-71.
20. Mahoney MG, Simpson A, Aho S, Uitto J, Pulkkinen L. Interspecies conservation and differential expression of mouse desmoglein gene family. *Exp Derm* 2002; 11:115-25.
21. Mahoney MG, Hu Y, Brennan D, Bazzi H, Christiano AM, Wahl K Jr. Delineation of diversified desmoglein distribution in stratified squamous epithelia: implications in diseases. *Exp Dermatol* 2006; 15:101-9.
22. Erb P, Ji J, Kump E, Mielgo A, Wernli M. Apoptosis and pathogenesis of melanoma and nonmelanoma skin cancer. *Adv Exp Med Biol* 2008; 624:283-95.
23. Chetty R, Serra S. Nuclear E-cadherin immunoreactivity: from biology to potential applications in diagnostic pathology. *Adv Anat Pathol* 2008; 15:234-40.
24. Salahshor S, Naidoo R, Serra S, Shih W, Tsao MS, Chetty R, Woodgett JR. Frequent accumulation of nuclear E-cadherin and alterations in the Wnt signaling pathway in esophageal squamous cell carcinomas. *Mod Pathol* 2008; 21:271-81.
25. Han AC, Soler AP, Tang CK, Knudsen KA, Salazar H. Nuclear localization of E-cadherin expression in Merkel cell carcinoma. *Arch Pathol Lab Med* 2000; 124:1147-51.
26. Wahl JK, Sacco PA, MaGrananah-Sadler TM, Sauppe LM, Wheelock MJ, Johnson KR. Plakoglobin domains that define its association with the desmosomal cadherins and the classical cadherins: identification of unique and shared domains. *J Cell Sci* 1996; 109:1143-54.
27. Wahl JK. Generation of monoclonal antibodies specific for desmoglein family members. *Hybrid Hybridomics* 2002; 21:37-44.
28. Mahoney MG, Tang W, Xiang MM, Moss SB, Gerton GL, Stanley JR, et al. Translocation of the zinc finger protein basonuclin from the mouse germ cell nucleus to the midpiece of the spermatozoon during spermiogenesis. *Biol Reprod* 1998; 59:388-94.
29. Brennan D, Hu Y, Kljuic A, Choi Y, Joubeh S, Bashkin M, et al. Differential structural properties and expression patterns suggest functional significance for multiple mouse desmoglein 1 isoforms. *Differentiation* 2004; 72:434-49.